

A MULTIDIMENSIONAL STUDY OF CLUSTERING IN THE REACTION $\pi^+p \rightarrow p\pi^+\pi^+\pi^-$ AT 8 GeV/c

H. BÖTTCHER, P. KOSTKA, K. LANIUS*, H. ROLOFF and H. SCHILLER
*Institut für Hochenergiephysik der Akademie der Wissenschaften der DDR,
Berlin-Zeuthen*

Received 25 April 1974
(Revised 1 August 1974)

Abstract A study of clustering of four-prong events is presented. The method used does not need any *a priori* knowledge about the reaction mechanisms involved. The classification of each event is done using the kinematical information contained in the whole sample of events. The clusters found are closely related to the main reaction mechanisms. The method is also easily applicable to other reaction channels.

1. Introduction

One of the important problems in high-energy physics is the theoretical and experimental study of multiparticle production. At increasing multiplicities conventional analysis using one- and two-dimensional projections of the phase space is no longer a powerful means to obtain detailed knowledge about the production mechanisms.

The Prism Plot Analysis (PPA) introduced by Pless and coworkers [1] was one of the first attempts to look into the full dimensional space of a few-body final state. Applying PPA one implicitly assumes that the events produced *via a priori* chosen subchannels form cluster(s) in the space of kinematical variables.

Based on the same hypothesis but opposite to PPA we start in our analysis with the search and separation of clusters of events in the phase space. The second step is the physical interpretation of the clusters found.

To find these clusters we used a method suggested by Koontz and Fukunaga [2]. This method does not need *a priori* knowledge about the clusters and uses for the classification of one event the kinematical information from the whole sample.

We apply this analysis to 4 400 events of the reaction

$$\pi^+p \rightarrow p\pi_f^+\pi_s^+\pi^- \quad (1)$$

* Now at JINR, Dubna.

at 8 GeV/c, where f/s denotes the fast/slow π^+ in the c.m.s. The experiment was done by the Aachen-Berlin-CERN Collaboration. Some results of a study of reaction (1) can be found in [3].

A description of the method is given in sect. 2. In sect. 3 we present the properties of the derived clusters. Conclusions are summarized in sect. 4.

2. Description of the method

2.1. Clustering algorithm

Koontz and Fukunaga [2] have formulated a non-parametric valley-seeking technique for cluster analysis (VST). The aim of any cluster analysis is the assignment of space points to classes according to some criteria e.g. the closeness of the points. The above-mentioned cluster algorithm is derived from the criterion which minimizes the information loss due to the replacement of vectors X_r (vector X_r being the kinematical variables defining the r th event) by a set of labels ω_r (cluster numbers).

A special solution of this problem is obtained by the application of the following procedure.

step 1: Choose an initial classification of events X_r *.

step 2: For each vector X_r count the numbers of vectors within a suitable chosen distance R of X_r that are assigned to each class.

step 3: Reclassify each X_r to the class with the largest number of members within the distance R of X_r .

step 4: If any vector is placed in a new class repeat from step 2. Otherwise stop.

That means by this procedure the number of points within R around X_r not belonging to the same class as X_r will be minimized. Therefore the boundary separating two classes moves away from the higher concentration towards valleys in the density distribution of the phase space.

In fig. 1 we illustrate the action of this procedure on a two dimensional data set. Fig. 1a shows the initial random assignment of the points to three classes. Fig. 1d gives as the result of the third iteration the final assignment (stable solution).

Since there is no clear definition of a cluster, the valley seeking technique is not really non-parametric. There are two parameters which one has to fix: firstly the number of classes N_c in the initial assignment, secondly the distance R . As shown in [2] the choice of N_c is not very crucial. As long as N_c is larger than the real number of clusters, unnecessary classes will become empty during the iteration (see fig. 1). The value of R is related to the most narrow valley to be searched for in the density

* In order to save computer time, our initial classification for reaction (1) was chosen not randomly but obtained by the following procedure: step 1.1 assign the events randomly to a given number of classes, step 1.2: for each class calculate the center of gravity, step 1.3: for each event determine the nearest center of gravity. Reclassify the event to the corresponding class; step 1.2 and 1.3 were repeated five times.

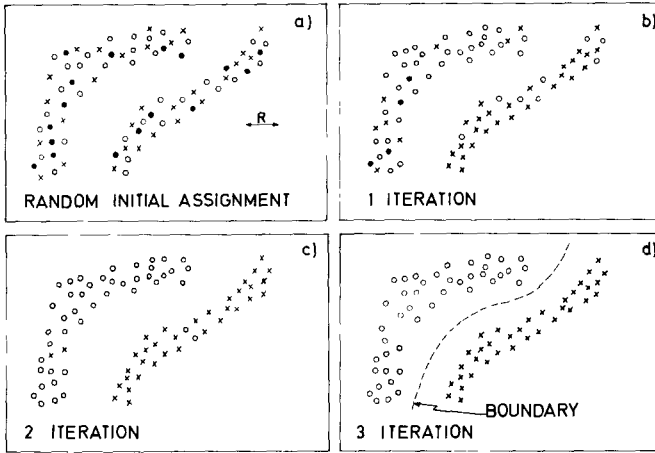


Fig. 1 Working scheme of the valley-seeking technique to find clusters illustrated at a two dimensional data set. The choice of R is indicated by the arrow (a) Random initial assignment of the points into three classes \circ , \times , \bullet . (b) Reassignment of the points after the 1st iteration. (c) Reassignment of the points after the 2nd iteration. (d) Final assignment of the points into two classes. One class has become empty during the iterations

distribution. In our analysis we fixed R by trial and error investigating the physical content of the clusters derived.

2.2 The data and analysis conditions

The method described above (VST) was applied to 4 400 events of the reaction (1). Some general characteristics of this channel are shown in figs. 2 and 3.

Each event of reaction (1) can be represented by 7 independent kinematical variables. In principle the choice of these variables is free. Since in reaction (1) resonance production is a dominant feature (fig. 2) we adopted as an obvious choice the following two sets

$$M(p\pi_f^+), M(p\pi_s^+), M(p\pi^-), M(\pi_f^+\pi^-), M(\pi_s^+\pi^-), \quad (2)$$

and

$$M^2(p\pi_f^+), M^2(p\pi_s^+), M^2(p\pi^-), M^2(\pi_f^+\pi^-), M^2(\pi_s^+\pi^-), \\ t(p/p), t(\pi^+/\pi^-). \quad (3)$$

M denotes the effective mass of the two particles enclosed in parentheses and t is the four-momentum transfer between the indicated particles. Starting from set (3) any set of independent invariants (masses squared and momentum transfers squared) can

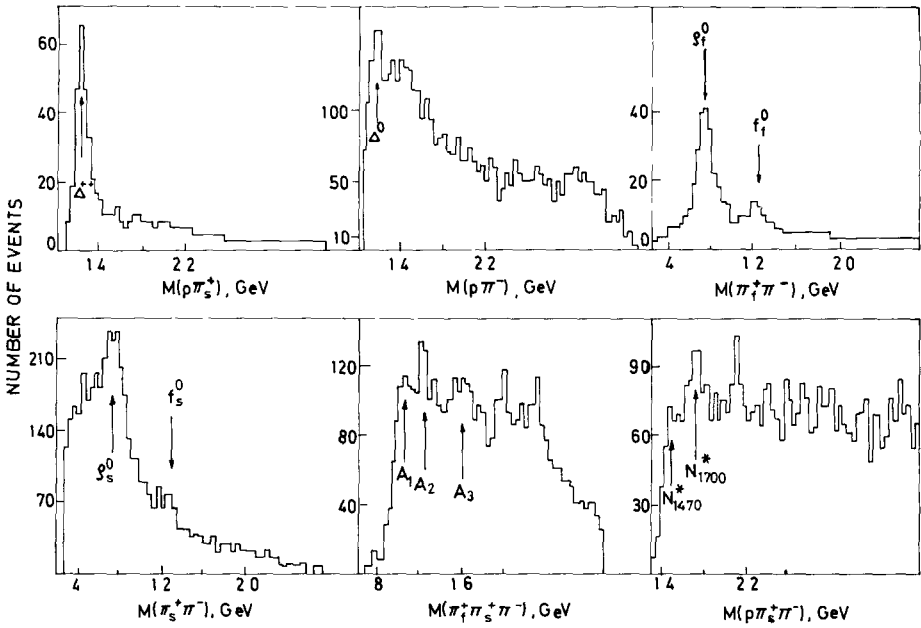


Fig. 2. Effective mass distributions derived from the reaction $\pi^+ p \rightarrow p \pi_f^+ \pi_s^+ \pi^-$ at 8 GeV/c, where f/s denotes the fast/slow π^+ in the c.m.s.

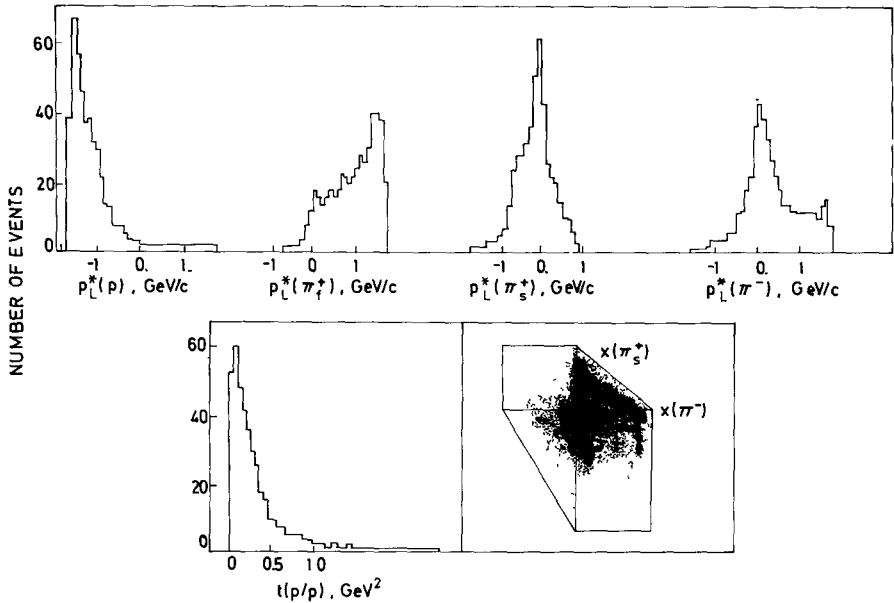


Fig. 3 Longitudinal momentum distributions of the final state particles in the c.m.s., the four-momentum transfer between the incoming and outgoing proton, and the LPS-plot of four-body $\pi^+ p$ interactions at 8 GeV/c.

Table 1

Population of the 10 clusters found for 4 400 events of reaction $\pi^+p \rightarrow p\pi^+\pi^+\pi^-$ at 8 GeV/c

Cluster	1	2	3	4	5	6	7	8	9	10
Events	1355	879	651	188	246	232	255	330	76	168

be obtained by linear transformations. Linear transformations are “cluster conserving”, since maxima/minima of the phase-space density are transformed into maxima/minima of the new density †.

The results of our analysis are obtained using the first set of variables. We found that these results could not be improved by using the second set. The reason for this could be twofold

- (i) The t values do not carry very much additional information about the clusters.
- (ii) Our limited statistics do not allow one to take advantage of the (in principle) better resolution of clusters offered by the increase of dimensions.

The most reasonable results were obtained with an R value of 0.455 GeV. Starting from 15 initial classes we got 10 significant clusters and the rest of 19 events. The population of the clusters is given in table 1.

We would like to mention that the cluster algorithm as well as the set of variables are ready for generalisation to higher multiplicities.

3. Results of the analysis

To see whether or not there is a correspondence between the clusters found and the subchannels (reaction mechanisms) known to govern reaction (1) we studied the main features in each cluster.

Cluster 1 (fig. 4). In the $M(p\pi_s^+)$ and $M(\pi_f^+\pi^-)$ distribution a clear Δ^{++} and ρ_f^0 respectively is seen. Neither the $(p\pi_s^+\pi^-)$ nor the $(\pi_f^+\pi_s^+\pi^-)$ mass distribution shows any resonance structure. Therefore in cluster 1 most of the events proceed $\nu\alpha$ ($\Delta^{++}\rho^0$) production.

Cluster 2 (fig. 5) Production of Δ^{++} can be observed in the $M(p\pi_s^+)$ distribution. Furthermore we see in both $(\pi^+\pi^-)$ mass combinations a $\rho_{f,s}^0$ and a $f_{f,s}^0$ signal. There are no other clear resonance signals.

Cluster 3 (fig. 6). Cluster 3 shows a mixture of Δ^{++} , f_f^0 , $N^*(1470)$ and $N^*(1700)$ production.

Cluster 4 (fig. 7). Again there is a clear Δ^{++} production and an indication of a $N^*(1700)$ signal. A remarkable feature in this cluster is the fact that the π^- is on average slower than the proton.

† We have checked that also a different set of variables like the components of the momenta in c.m.s leads to clusters corresponding to subchannels.

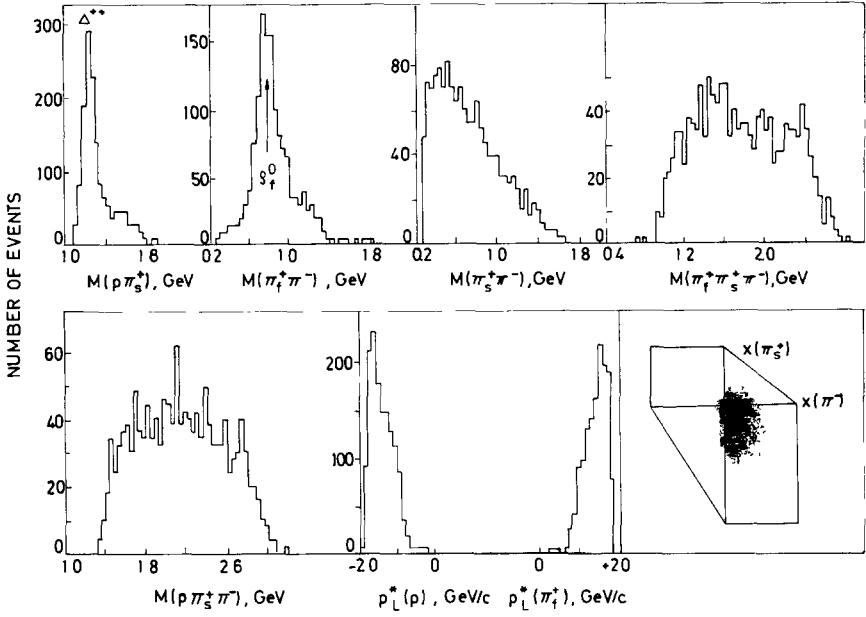


Fig. 4. Effective mass distributions, longitudinal momentum distributions, and LPS-plot characterizing cluster 1

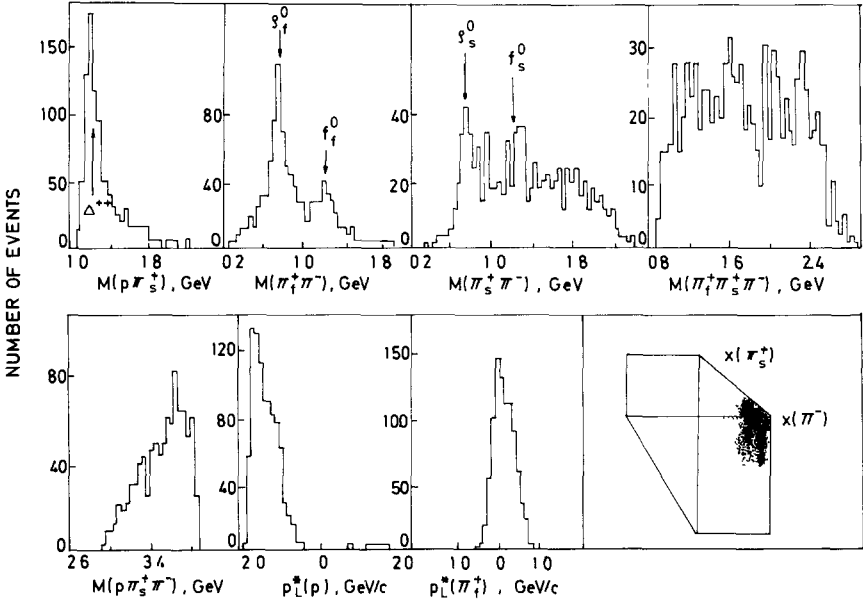


Fig. 5. Effective mass distributions, longitudinal momentum distributions, and LPS-plot characterizing cluster 2.

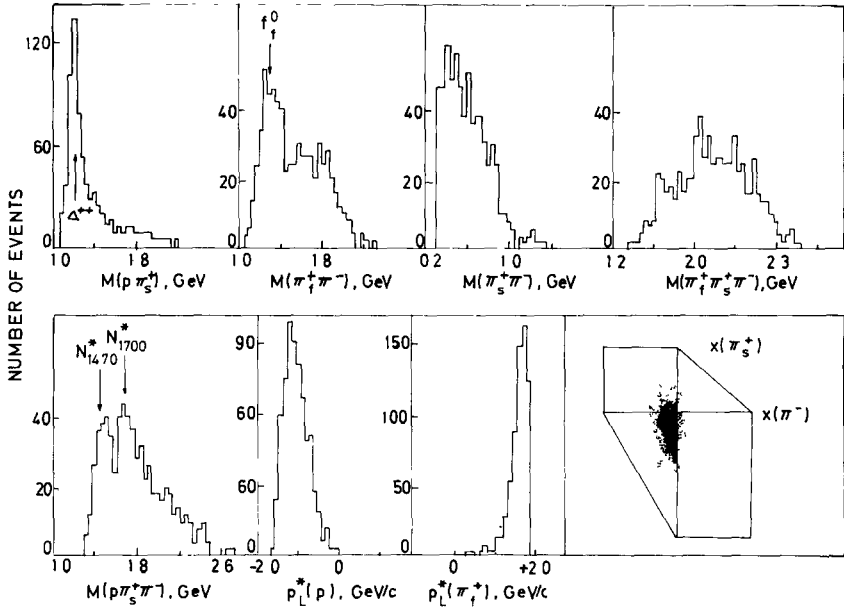


Fig. 6 Effective mass distributions, longitudinal momentum distributions, and LPS-plot characterizing cluster 3.

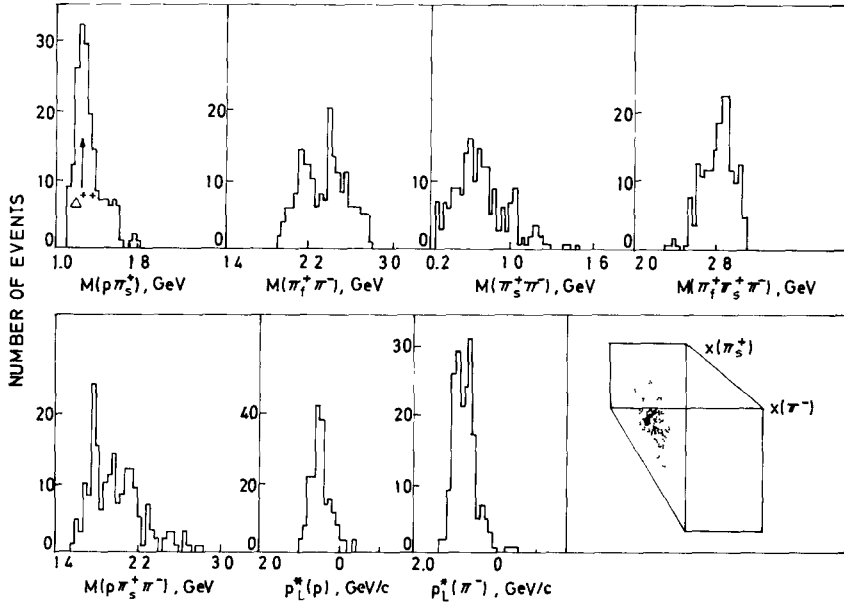


Fig. 7 Effective mass distributions, longitudinal momentum distributions, and LPS-plot characterizing cluster 4.

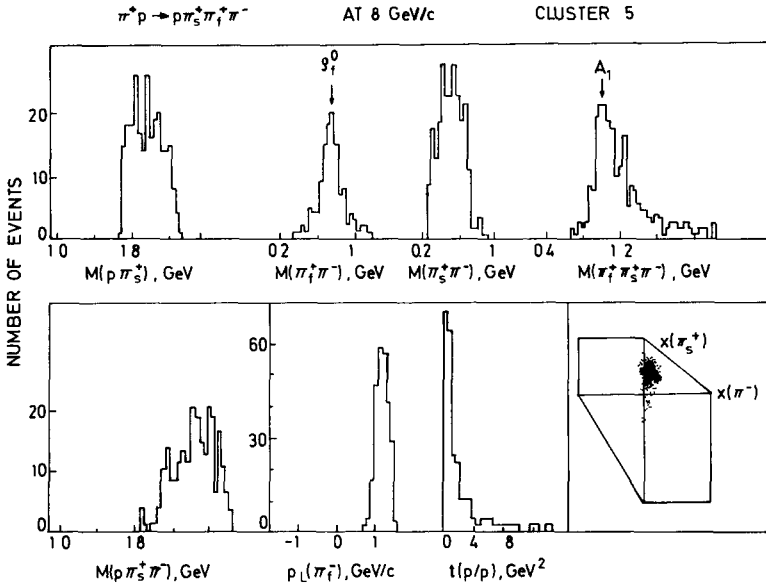


Fig. 8 Effective mass distributions, longitudinal momentum distribution of the π_f^+ , the four-momentum transfer between the incoming and outgoing proton, and the LPS-plot characterizing cluster 5.

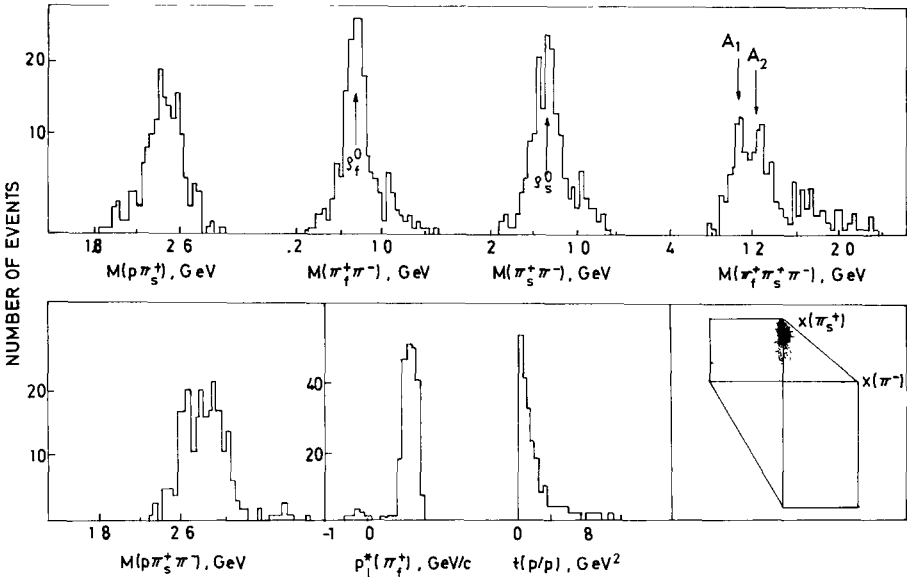


Fig. 9. Effective mass distributions, longitudinal momentum distribution of the π_f^+ , the four-momentum transfer between the incoming and outgoing proton, and the LPS-plot characterizing cluster 6.

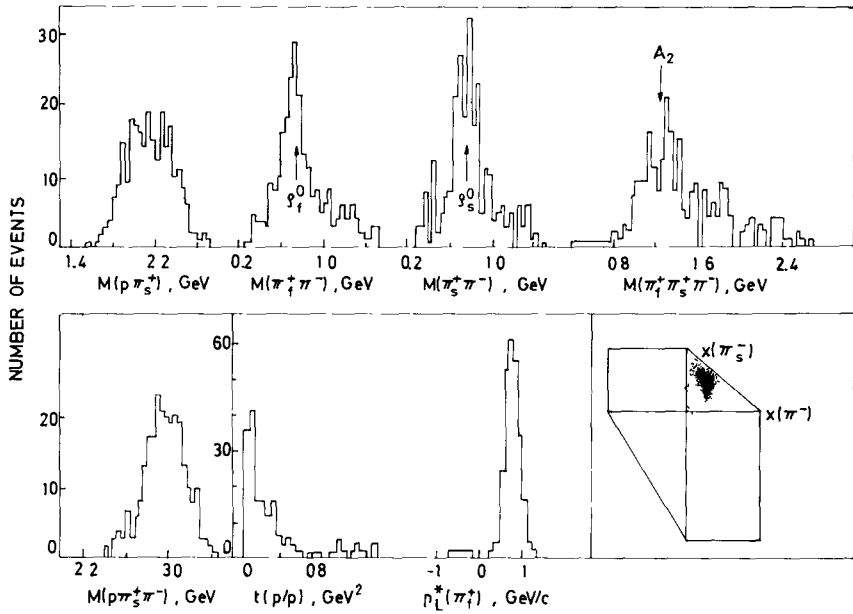


Fig. 10 Effective mass distributions, longitudinal momentum distribution of the π_f^+ , the four-momentum transfer between the incoming and outgoing proton, and the LPS-plot characterizing cluster 7.

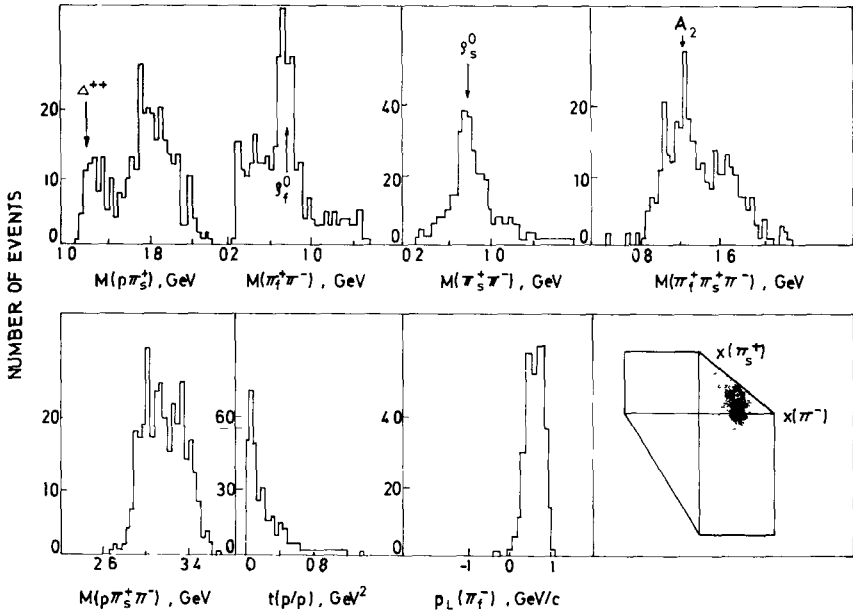


Fig. 11 Effective mass distributions, longitudinal momentum distribution of the π_f^+ , the four-momentum transfer between the incoming and outgoing proton, and the LPS-plot characterizing cluster 8.

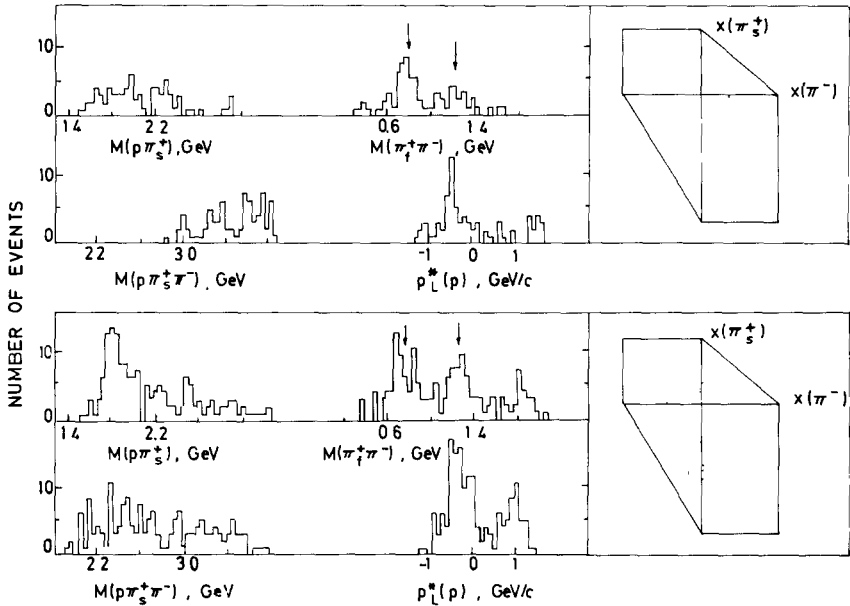


Fig. 12. Effective mass distributions, longitudinal momentum distributions of the proton, and the LPS-plot characterizing cluster 9 and cluster 10

Cluster 5 (fig. 8). A clear signal in the A_1 mass region is seen. This (3π) system decays mainly via (ρ_f^0, π) . The $t(p/p)$ distribution supports the interpretation of this cluster being A_1 production.

Cluster 6 (fig. 9). Production of ρ^0 is seen in both $(\pi^+\pi^-)$ combinations and peaks are visible in the A_1, A_2 region of the three pion distribution.

Cluster 7 (fig. 10). This cluster is quite similar to cluster 6. However, in the A_1 region there is only a shoulder.

Cluster 8 (fig. 11). Cluster 8 shows a rather clear A_2 signal and a ρ^0 in both $(\pi^+\pi^-)$ combinations. The broad $t(p/p)$ distribution with its turnover is quite different compared to that of cluster 5 (A_1 production). In addition some Δ^{++} is seen.

Clusters 9, 10 (fig. 12). The striking feature of these clusters is the large average value of $p_L^*(p)$. In the fast $(\pi^+\pi^-)$ combination, ρ^0 and f^0 signals can be seen.

A remarkable feature of all clusters found in the space of five two-particle masses is that they populate connected areas in the LPS plot. These areas are situated to a large extent in those regions which one would select in a LPS analysis to separate the corresponding subchannels.

The resonance content observed in each cluster is summarized in table 2. It can be seen that one subchannel can give rise to more than one cluster and that some clusters still contain contributions from more than one subchannel. The situation is roughly sketched in fig. 13. The overlapping clusters produced by different subchan-

Table 2

Resonance content of the 10 clusters found for 4 400 events of reaction $\pi^+p \rightarrow p\pi_f^+\pi_s^+\pi^-$ at 8 GeV/c (f/s denotes the fast/slow π^+ in the c.m.s)

Cluster	$\Delta^{++}(1236)$	$\Delta^0(1236)$	ρ_f^0	f_f	ρ_s^0	f_s	$N^*(1470)$	$N^*(1700)$	A_1	A_2
1	x		x							
2	x		x	x	x	x				
3	x	?		x			x	x		
4	x							?		
5			x						x	
6			x		x				x	x
7			x		x				?	x
8			x		x					x
9/10			x		x					

nels could be due to the relatively low energy ($p_{lab} = 8 \text{ GeV}/c$). Therefore it seems worthwhile to us to apply this analysis at higher energies.

To study e.g. the $(\Delta^{++}\rho^0)$ production, table 2 and fig. 13 suggest combination of clusters 1 and 2. Fig. 14 shows the main characteristics of the combined cluster. It should be mentioned that without combining these two clusters the decay angular distribution of the ρ^0 would be highly asymmetric. The shape of the decay angular distribution explains why the $(\Delta^{++}\rho^0)$ subchannel forms two clusters the peripherality of the ρ^0 production together with its decay angular distribution leads to a broad valley in the $(p\pi^-)$ mass distribution (see fig. 15). The cluster algorithm by its construction splits the whole subchannel into two clusters

As can be seen from the $(\pi_f^+\pi^-)$ mass distribution in fig. 14 the combined cluster 1 + 2 still contains contributions from other subchannels. In order to extract the $(\Delta^{++}\rho^0)$ cross section the "mass slice method" [4] was used. We obtained the value $\sigma(\Delta^{++}\rho^0) = (406 \pm 28) \mu\text{b}$ which is in good agreement with the published values [3, 5]

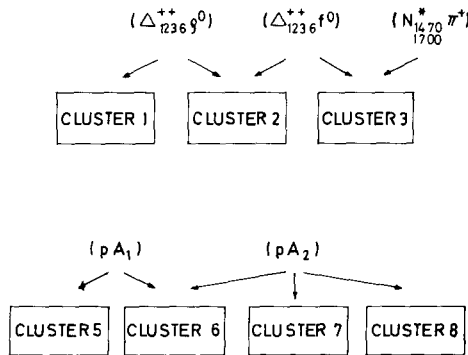


Fig. 13. Schematic view of the overlapping of contributions coming from the subchannels $(\Delta^{++}(1236)\rho^0)$, $(\Delta^{++}(1236)f^0)$, $(N^*(1470)\pi^+)$ to cluster 1, 2 and 3 and from the subchannels (pA_1) , (pA_2) to cluster 5, 6, 7 and 8.

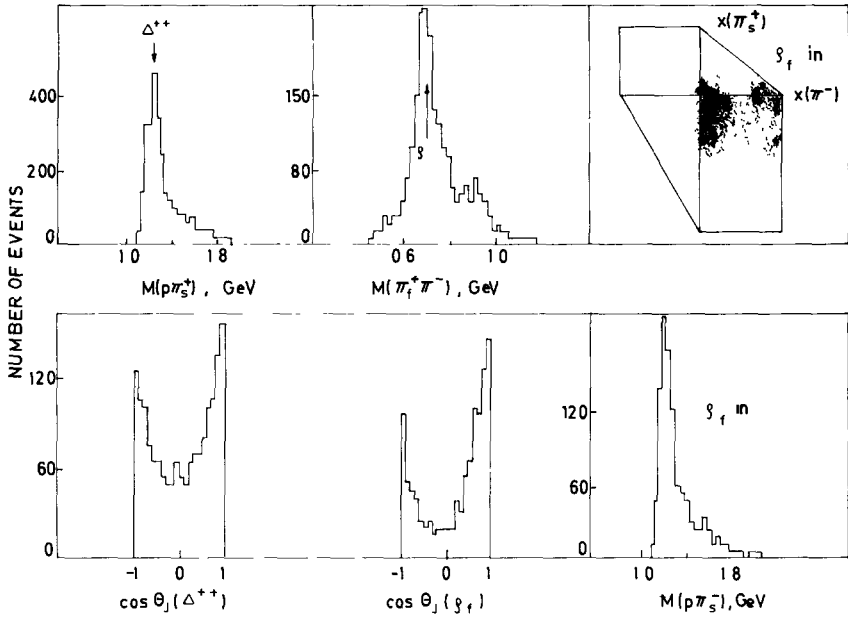


Fig. 14. Effective mass distributions, decay angular distributions and the LPS plot characterizing the $(\Delta^{++}(1236)\rho^0)$ production in the combined cluster 1 and 2

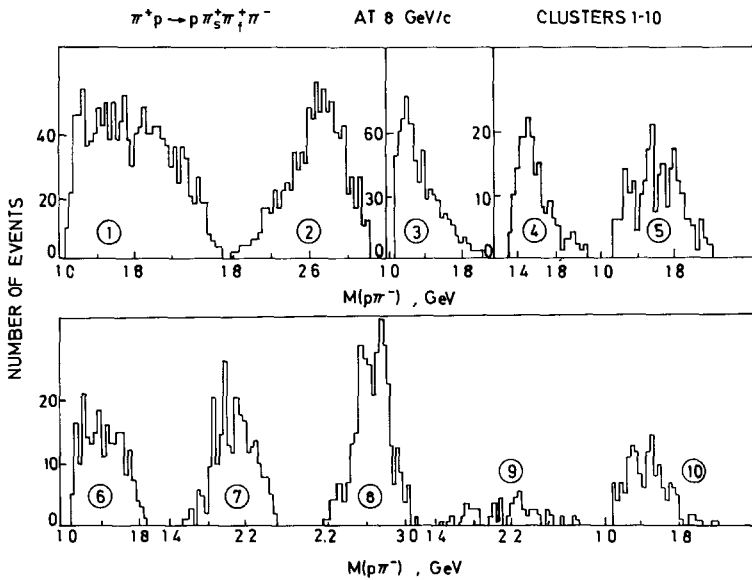


Fig. 15. The $(p\pi^-)$ effective mass distributions for all clusters separately.

4. Conclusion

We have presented a study of clustering of four-prong events produced in π^+p interactions at 8 GeV/c. The method used does not need any *a priori* knowledge about the reaction mechanisms involved.

- (i) There are cluster of events in the phase space.
- (ii) These clusters, found by a purely statistical method, have correspondence to dynamical mechanisms.
- (iii) There are still clusters to which more than one mechanism contribute.
- (iv) For some mechanisms the method offers a good separation.
- (v) The method is applicable to a great variety of final states.

We are deeply indebted to the ABC-Collaboration which supplied the data. We wish to thank Drs. J. Kaltwasser, L. Becker and Ch. Spiering for valuable discussions.

References

- [1] J.E. Bran, M.F. Hodons, I.A. Pless and R.A. Singer, Phys. Rev. Letters 27 (1971) 1181.
- [2] W.L. Koontz and K. Fukunaga, IEEE Transactions on computers, C-21 (1972) 2.
- [3] M. Aderholz et al., Nucl. Phys. B8 (1968) 45.
- [4] M. Aguilar-Benitez et al., Phys. Rev. 6 (1972) 29.
- [5] E. Bracci et al., CERN/HERA 72-1.